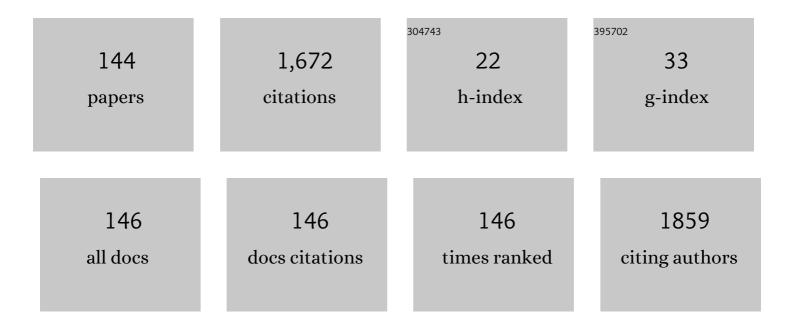
List of Publications by Year in descending order

Source: https://exaly.com/author-pdf/5186979/publications.pdf Version: 2024-02-01



IFA-CIIN DADK

| #  | Article  | IF   | CITATIONS |
|----|--|------|-----------|
| 1  | Multilevel Nonvolatile Small-Molecule Memory Cell Embedded with Ni Nanocrystals Surrounded by a<br>NiO Tunneling Barrier. Nano Letters, 2009, 9, 1713-1719.  | 9.1  | 103       |
| 2  | Super Ultra-High Resolution Liquid-Crystal-Display Using Perovskite Quantum-Dot Functional Color-Filters. Scientific Reports, 2018, 8, 12881.  | 3.3  | 57        |
| 3  | Effect of NiOx thin layer fabricated by oxygen-plasma treatment on polymer photovoltaic cell. Solar<br>Energy Materials and Solar Cells, 2010, 94, 1591-1596.  | 6.2  | 50        |
| 4  | Effect of Interface Thickness on Power Conversion Efficiency of Polymer Photovoltaic Cells.<br>Electronic Materials Letters, 2009, 5, 47-50.   | 2.2  | 44        |
| 5  | Effect of Metal-Reflection and Surface-Roughness Properties on Power-Conversion Efficiency for Polymer Photovoltaic Cells. Journal of Physical Chemistry C, 2009, 113, 21915-21920.  | 3.1  | 43        |
| 6  | Effects of Abrasive Morphology and Surfactant Concentration on Polishing Rate of Ceria Slurry.<br>Japanese Journal of Applied Physics, 2003, 42, 1150-1153.  | 1.5  | 42        |
| 7  | Effect of core quantum-dot size on power-conversion-efficiency for silicon solar-cells implementing energy-down-shift using CdSe/ZnS core/shell quantum dots. Nanoscale, 2014, 6, 12524-12531.   | 5.6  | 41        |
| 8  | Influence of the electrokinetic behaviors of abrasive ceria particles and the deposited<br>plasma-enhanced tetraethylorthosilicate and chemically vapor deposited<br>Si <sub>3</sub> N <sub>4</sub> films in an aqueous medium on chemical mechanical planarization for<br>shallow trench isolation. Journal of Materials Research, 2003, 18, 2163-2169. | 2.6  | 37        |
| 9  | Effect of double MgO tunneling barrier on thermal stability and TMR ratio for perpendicular MTJ spin-valve with tungsten layers. Applied Physics Letters, 2016, 109, .   | 3.3  | 36        |
| 10 | Oneâ€Pot Gramâ€Scale, Ecoâ€Friendly, and Costâ€Effective Synthesis of CuGaS <sub>2</sub> /ZnS Nanocrystals as Efficient UVâ€Harvesting Downâ€Converter for Photovoltaics. Advanced Energy Materials, 2018, 8, 1703418.   | 19.5 | 36        |
| 11 | Continuous Separation of Circulating Tumor Cells from Whole Blood Using a Slanted Weir<br>Microfluidic Device. Cancers, 2019, 11, 200.   | 3.7  | 36        |
| 12 | Solar cell implemented with silicon nanowires on pyramid-texture silicon surface. Solar Energy, 2013, 91, 256-262.   | 6.1  | 33        |
| 13 | Enhanced efficiency and current density of solar cells via energy-down-shift having<br>energy-tuning-effect of highly UV-light-harvesting Mn2+-doped quantum dots. Nano Energy, 2017, 33,<br>257-265.  | 16.0 | 33        |
| 14 | Surfactant Effect on Oxide-to-Nitride Removal Selectivity of Nano-abrasive Ceria Slurry for Chemical<br>Mechanical Polishing. Japanese Journal of Applied Physics, 2003, 42, 5420-5425.  | 1.5  | 32        |
| 15 | Effect of iron(III) nitrate concentration on tungsten chemical-mechanical-planarization performance.<br>Applied Surface Science, 2013, 282, 512-517.   | 6.1  | 29        |
| 16 | Role of Hydrogen Peroxide in Alkaline Slurry on the Polishing Rate of Polycrystalline Ge[sub 2]Sb[sub<br>2]Te[sub 5] Film in Chemical Mechanical Polishing. Electrochemical and Solid-State Letters, 2010, 13,<br>H155.  | 2.2  | 28        |
| 17 | Electro-Forming and Electro-Breaking of Nanoscale Ag Filaments for Conductive-Bridging<br>Random-Access Memory Cell using Ag-Doped Polymer-Electrolyte between Pt Electrodes. Scientific<br>Reports, 2017, 7, 3065.  | 3.3  | 28        |
| 18 | Impact of donor, acceptor, and blocking layer thickness on power conversion efficiency for small-molecular organic solar cells. Synthetic Metals, 2009, 159, 1705-1709.  | 3.9  | 27        |

| #  | Article   | IF   | CITATIONS |
|----|---|------|-----------|
| 19 | Effects of Pt capping layer on perpendicular magnet anisotropy in pseudo-spin valves of<br>Ta/CoFeB/MgO/CoFeB/Pt magnetic-tunneling junctions. Applied Physics Letters, 2013, 102, .  | 3.3  | 27        |
| 20 | The dependency of tunnel magnetoresistance ratio on nanoscale thicknesses of<br>Co <sub>2</sub> Fe <sub>6</sub> B <sub>2</sub> free and pinned layers for<br>Co <sub>2</sub> Fe <sub>6</sub> B <sub>2</sub> /MgO-based perpendicular-magnetic-tunnel-junctions.<br>Nanoscale, 2015, 7, 8142-8148. | 5.6  | 26        |
| 21 | Influence of Physical Characteristics of Ceria Particles on Polishing Rate of Chemical Mechanical<br>Planarization for Shallow Trench Isolation. Japanese Journal of Applied Physics, 2004, 43, 7427-7433.  | 1.5  | 23        |
| 22 | Effect of Molecular Weight of Surfactant in Nano Ceria Slurry on Shallow Trench Isolation<br>Chemical Mechanical Polishing (CMP). Japanese Journal of Applied Physics, 2004, 43, L1060-L1063.   | 1.5  | 23        |
| 23 | The energy-down-shift effect of Cd <sub>0.5</sub> Zn <sub>0.5</sub> S–ZnS core–shell quantum dots<br>on power-conversion-efficiency enhancement in silicon solar cells. Physical Chemistry Chemical<br>Physics, 2014, 16, 18205.  | 2.8  | 23        |
| 24 | Nanoscale CuO solid-electrolyte-based conductive-bridging-random-access-memory cell operating multi-level-cell and 1selector1resistor. Journal of Materials Chemistry C, 2015, 3, 9540-9550.  | 5.5  | 21        |
| 25 | Dependency of Tunneling-Magnetoresistance Ratio on Nanoscale Spacer Thickness and Material for<br>Double MgO Based Perpendicular-Magnetic-Tunneling-Junction. Scientific Reports, 2016, 6, 38125.   | 3.3  | 21        |
| 26 | Effects of the Physical Characteristics of Cerium Oxide on Plasma-Enhanced Tetraethylorthosiliate<br>Removal Rate of Chemical Mechanical Polishing for Shallow Trench Isolation. Japanese Journal of<br>Applied Physics, 2003, 42, 1227-1230.   | 1.5  | 20        |
| 27 | Atomic force microscopy study of the role of molecular weight of poly(acrylic acid) in chemical mechanical planarization for shallow trench isolation. Journal of Materials Research, 2006, 21, 473-479.  | 2.6  | 20        |
| 28 | Crystalline structure of ceria particles controlled by the oxygen partial pressure and STI CMP performances. Ultramicroscopy, 2008, 108, 1292-1296.   | 1.9  | 20        |
| 29 | Highly Enhanced TMR Ratio and Δ for Double MgO-based p-MTJ Spin-Valves with Top Co2Fe6B2 Free Layer<br>by Nanoscale-thick Iron Diffusion-barrier. Scientific Reports, 2017, 7, 11907.   | 3.3  | 20        |
| 30 | Flexible conductive-bridging random-access-memory cell vertically stacked with top Ag electrode,<br>PEO, PVK, and bottom Pt electrode. Nanotechnology, 2014, 25, 435204.  | 2.6  | 19        |
| 31 | Perpendicular magnetic tunnel junction (p-MTJ) spin-valves designed with a top Co2Fe6B2 free layer and a nanoscale-thick tungsten bridging and capping layer. NPG Asia Materials, 2016, 8, e324-e324.   | 7.9  | 18        |
| 32 | Increase in the Adsorption Density of Anionic Molecules on Ceria for Defect-Free STI CMP. Journal of the Electrochemical Society, 2010, 157, H72.   | 2.9  | 17        |
| 33 | Potassium Permanganate as Oxidizer in Alkaline Slurry for Chemical Mechanical Planarization of<br>Nitrogen-doped Polycrystalline Ge[sub 2]Sb[sub 2]Te[sub 5] Film. Journal of the Electrochemical<br>Society, 2010, 157, H1036.   | 2.9  | 17        |
| 34 | Effects of Grain Size and Abrasive Size of Polycrystalline Nano-particle Ceria Slurry on Shallow<br>Trench Isolation Chemical Mechanical Polishing. Japanese Journal of Applied Physics, 2004, 43,<br>L365-L368.  | 1.5  | 16        |
| 35 | Effects of abrasive particle size and molecular weight of poly(acrylic acid) in ceria slurry on removal selectivity of SiO2/Si3N4 films in shallow trench isolation chemical mechanical planarization. Journal of Materials Research, 2007, 22, 777-787.  | 2.6  | 16        |
| 36 | Low-cost and flexible ultra-thin silicon solar cell implemented with energy-down-shift via<br>Cd <sub>0.5</sub> Zn <sub>0.5</sub> S/ZnS core/shell quantum dots. Journal of Materials Chemistry A,<br>2015, 3, 481-487.   | 10.3 | 16        |

| #  | Article  | IF  | CITATIONS |
|----|--|-----|-----------|
| 37 | Constraints on removal of Si <sub>3</sub> N <sub>4</sub> film with conformation-controlled<br>poly(acrylic acid) in shallow-trench isolation chemical–mechanical planarization (STI CMP). Journal<br>of Materials Research, 2008, 23, 49-54.   | 2.6 | 15        |
| 38 | Effect of Hydroxyethyl Cellulose Concentration on Surface Qualities of Silicon Wafer after Touch Polishing Process. Electrochemical and Solid-State Letters, 2010, 13, H147.   | 2.2 | 15        |
| 39 | Chemical Mechanical Planarization Mechanism for Nitrogen-Doped Polycrystalline<br>Ge <sub>2</sub> Sb <sub>2</sub> Te <sub>5</sub> Film Using Nitric Acidic Slurry Added with Hydrogen<br>Peroxide. Journal of the Electrochemical Society, 2011, 158, H666-H670.   | 2.9 | 15        |
| 40 | Double MgO-based Perpendicular Magnetic-Tunnel-Junction Spin-valve Structure with a Top Co2Fe6B2<br>Free Layer using a Single SyAF [Co/Pt]n Layer. Scientific Reports, 2018, 8, 2139.  | 3.3 | 15        |
| 41 | Dependence of Nanotopography Impact on Abrasive Size and Surfactant Concentration in Ceria Slurry<br>for Shallow Trench Isolation Chemical Mechanical Polishing. Japanese Journal of Applied Physics,<br>2004, 43, L1-L4.  | 1.5 | 13        |
| 42 | Tunneling-Magnetoresistance Ratio Comparison of MgO-Based<br>Perpendicular-Magnetic-Tunneling-Junction Spin Valve Between Top and Bottom Co2Fe6B2 Free Layer<br>Structure. Nanoscale Research Letters, 2016, 11, 433.  | 5.7 | 13        |
| 43 | Effect of abrasive material properties on polishing rate selectivity of nitrogen-doped<br>Ge <sub>2</sub> Sb <sub>2</sub> Te <sub>5</sub> to SiO <sub>2</sub> film in chemical mechanical<br>polishing. Journal of Materials Research, 2008, 23, 3323-3329.  | 2.6 | 12        |
| 44 | Effects of metallic contaminant type and concentration on photovoltaic performance degradation of p-type silicon solar cells. Journal of the Korean Physical Society, 2013, 63, 47-52.   | 0.7 | 12        |
| 45 | Effects of the radio-frequency sputtering power of an MgO tunneling barrier on the tunneling magneto-resistance ratio for Co <sub>2</sub> Fe <sub>6</sub> B <sub>2</sub> /MgO-based perpendicular-magnetic tunnel junctions. Journal of Materials Chemistry C, 2016, 4, 135-141.   | 5.5 | 12        |
| 46 | Interfacial Chemical and Mechanical Reactions between Tungsten-Film and Nano-Scale Colloidal<br>Zirconia Abrasives for Chemical-Mechanical-Planarization. ECS Journal of Solid State Science and<br>Technology, 2020, 9, 054001.   | 1.8 | 12        |
| 47 | Spectral Analyses on Pad Dependency of Nanotopography Impact on Oxide Chemical Mechanical Polishing. Japanese Journal of Applied Physics, 2002, 41, L17-L19.   | 1.5 | 11        |
| 48 | Dependence of pH, Molecular Weight, and Concentration of Surfactant in Ceria Slurry on Saturated<br>Nitride Removal Rate in Shallow Trench Isolation Chemical Mechanical Polishing. Japanese Journal of<br>Applied Physics, 2005, 44, 4752-4758.   | 1.5 | 11        |
| 49 | Correlation of the structural properties of a Pt seed layer with the perpendicular magnetic<br>anisotropy features of full Heusler-based Co2FeAl/MgO/Co2Fe6B2 junctions via a 12-inch scale Si wafer<br>process. Applied Physics Letters, 2013, 103, .   | 3.3 | 11        |
| 50 | Double Pinned Perpendicular-Magnetic-Tunnel-Junction Spin-Valve Providing Multi-level Resistance<br>States. Scientific Reports, 2019, 9, 11932.  | 3.3 | 11        |
| 51 | Dishing-free chemical mechanical planarization for copper films. Colloids and Surfaces A:<br>Physicochemical and Engineering Aspects, 2021, 616, 126143.   | 4.7 | 11        |
| 52 | Dependency of anti-ferro-magnetic coupling strength on Ru spacer thickness of<br>[Co/Pd]n-synthetic-anti-ferro-magnetic layer in perpendicular magnetic-tunnel-junctions fabricated on<br>12-inch TiN electrode wafer. Journal of Applied Physics, 2014, 116, .  | 2.5 | 10        |
| 53 | Influence of face-centered-cubic texturing of Co <sub>2</sub> Fe <sub>6</sub> B <sub>2</sub> pinned<br>layer on tunneling magnetoresistance ratio decrease in<br>Co <sub>2</sub> Fe <sub>6</sub> B <sub>2</sub> /MgO-based p-MTJ spin valves stacked with a<br>[Co/Pd] <sub>n</sub> -SvAF layer. Nanotechnology. 2015. 26. 195702. | 2.6 | 10        |
| 54 | Effects of Abrasive Size and Surfactant Concentration on the Non-Prestonian Behavior of Ceria<br>Slurry in Shallow Trench Isolation Chemical Mechanical Polishing. Japanese Journal of Applied<br>Physics, 2005, 44, L136-L139.  | 1.5 | 9         |

| #  | Article  | IF  | CITATIONS |
|----|--|-----|-----------|
| 55 | Extremely proximity gettering for semiconductor devices. Materials Science and Engineering B:<br>Solid-State Materials for Advanced Technology, 2006, 134, 249-256.  | 3.5 | 9         |
| 56 | Impact of the top silicon thickness on phonon-limited electron mobility in (110)-oriented<br>ultrathin-body silicon-on-insulator n-metal-oxide-semiconductor field-effect transistors. Journal of<br>Applied Physics, 2007, 102, 063520.   | 2.5 | 9         |
| 57 | Dependence of memory margin of Cap-less memory cells on top Si thickness. Applied Physics Letters, 2009, 94, 023508.   | 3.3 | 9         |
| 58 | Co <sub>2</sub> Fe <sub>6</sub> B <sub>2</sub> /MgO-based perpendicular spin-transfer-torque<br>magnetic-tunnel-junction spin-valve without [Co/Pt] <sub> <i>n</i> </sub> lower<br>synthetic-antiferromagnetic layer. Nanotechnology, 2015, 26, 475705.                                  | 2.6 | 9         |
| 59 | Novel quantum dot enhancement film with a super-wide color gamut for LCD displays. Journal of the<br>Korean Physical Society, 2018, 72, 45-51.   | 0.7 | 9         |
| 60 | Highly Selective Polishing Rate Between a Tungsten Film and a Silicon-Dioxide Film by Using a<br>Malic-Acid Selectivity Agent in Tungsten-Film Chemical-Mechanical Planarization. Journal of the<br>Korean Physical Society, 2020, 76, 1127-1132.  | 0.7 | 9         |
| 61 | Dependence of crystal nature on the gettering efficiency of iron and nickel in a Czochralski silicon wafer. Microelectronic Engineering, 2003, 66, 247-257.  | 2.4 | 8         |
| 62 | Dependence of temperature and self-heating on electron mobility in ultrathin body<br>silicon-on-insulator n-metal-oxide-semiconductor field-effect transistors. Journal of Applied Physics,<br>2008, 103, .  | 2.5 | 8         |
| 63 | Multiselectivity Chemical Mechanical Polishing for NAND Flash Memories beyond 32 nm. Journal of the Electrochemical Society, 2010, 157, H607.  | 2.9 | 8         |
| 64 | Dependence of nonvolatile memory characteristics on curing temperature for polymer memory-cell embedded with Au nanocrystals in poly(N-vinylcarbazole). Current Applied Physics, 2011, 11, e25-e29.  | 2.4 | 8         |
| 65 | Polymer photovoltaic cell embedded with p-type single walled carbon nanotubes fabricated by spray process. Nanotechnology, 2012, 23, 325401.   | 2.6 | 8         |
| 66 | Highly enhanced perpendicular magnetic anisotropic features in a CoFeB/MgO free layer via WN<br>diffusion barrier. Acta Materialia, 2016, 110, 217-225.  | 7.9 | 8         |
| 67 | A two-terminal perpendicular spin-transfer torque based artificial neuron. Journal Physics D: Applied Physics, 2018, 51, 504002.   | 2.8 | 8         |
| 68 | Influence of Scavenger on Abrasive Stability Enhancement and Chemical and Mechanical Properties<br>for Tungsten-Film Chemical- Mechanical-Planarization. ECS Journal of Solid State Science and<br>Technology, 2020, 9, 065001.  | 1.8 | 8         |
| 69 | Strained Si engineering for nanoscale MOSFETs. Materials Science and Engineering B: Solid-State<br>Materials for Advanced Technology, 2006, 134, 142-153.  | 3.5 | 7         |
| 70 | Effect of Calcination Process on Synthesis of Ceria Particles, and Its Influence on Shallow Trench<br>Isolation Chemical Mechanical Planarization Performance. Japanese Journal of Applied Physics, 2006,<br>45, 4893-4897.  | 1.5 | 7         |
| 71 | Dependence of Electrical Characteristics on Si Thickness and Ge Concentration for Unstrained Si<br>Grown on Strained SiGe-on-Insulator n-Metal–Oxide–Semiconductor Field-Effect Transistor. Japanese<br>Journal of Applied Physics, 2007, 46, 3324-3329.                                 | 1.5 | 7         |
| 72 | Comparative study of self-heating effect on electron mobility in nano-scale strained<br>silicon-on-insulator and strained silicon grown on relaxed SiGe-on-insulator<br>n-metal–oxide–semiconductor field-effect transistors. Semiconductor Science and Technology, 2009,<br>24, 035014. | 2.0 | 7         |

| #  | Article  | IF  | CITATIONS |
|----|--|-----|-----------|
| 73 | Effect of Slurry pH and H2O2on Polycrystalline Ge2Sb2Te5CMP Performance. Journal of the Electrochemical Society, 2012, 159, C546-C551.   | 2.9 | 7         |
| 74 | Effect of Potassium Ferricyanide in the Acid Solution on Performance of Tungsten Chemical Mechanical Planarization. Journal of the Electrochemical Society, 2012, 159, H363-H366.  | 2.9 | 7         |
| 75 | Dependency of tunneling magneto-resistance on Fe insertion-layer thickness in Co2Fe6B2/MgO-based magnetic tunneling junctions. Journal of Applied Physics, 2015, 117, .  | 2.5 | 7         |
| 76 | Design of two-terminal-electrode vertical thyristor as cross-point memory cell without selector.<br>Applied Physics Letters, 2018, 113, .  | 3.3 | 7         |
| 77 | Effect of a Co-evaporated Alq3:Liq cathode buffer layer on the performance of a polymer photovoltaic cell. Journal of the Korean Physical Society, 2015, 66, 1872-1878.  | 0.7 | 6         |
| 78 | Dependency of tunneling magnetoresistance ratio on Pt seed-layer thickness for double MgO<br>perpendicular magnetic tunneling junction spin-valves with a top<br>Co <sub>2</sub> Fe <sub>6</sub> B <sub>2</sub> free layer <i>ex-situ</i> annealed at 400 °C.<br>Nanotechnology, 2016, 27, 485203. | 2.6 | 6         |
| 79 | Extended Defects and Pile-Up of Interstitial Oxygen in Silicon Wafer Due to MeV-Level Nitrogen Ion<br>Implantation. Japanese Journal of Applied Physics, 2004, 43, 6854-6857.  | 1.5 | 5         |
| 80 | Silicon thickness fluctuation scattering dependence of electron mobility in ultrathin body<br>silicon-on-insulator n-metal-oxide-semiconductor field-effect transistors. Journal of Applied Physics,<br>2008, 103, 084503.   | 2.5 | 5         |
| 81 | The effect of donor layer thickness on the power conversion efficiency of organic photovoltaic devices fabricated with a double small-molecular layer. Nanotechnology, 2009, 20, 335201.   | 2.6 | 5         |
| 82 | Nonvolatile memory characteristics of small-molecule memory cells with electron-transport and hole-transport bilayers. Current Applied Physics, 2010, 10, e37-e41.   | 2.4 | 5         |
| 83 | Micro Defect Size in Si Single Crystal Grown by Czochralski Method. Japanese Journal of Applied<br>Physics, 2010, 49, 121301.  | 1.5 | 5         |
| 84 | Effect of coupling ability between a synthetic antiferromagnetic layer and pinned layer on a bridging<br>layer of Ta, Ti, and Pt in perpendicular-magnetic tunnel junctions. Nanotechnology, 2016, 27, 295705.   | 2.6 | 5         |
| 85 | An electroforming-free mechanism for Cu <sub>2</sub> O solid-electrolyte-based conductive-bridge random access memory (CBRAM). Journal of Materials Chemistry C, 2020, 8, 8125-8134.   | 5.5 | 5         |
| 86 | Effect of O2 Plasma Treatment on Hole-Injection Enhancement for Organic Light-Emitting Devices with Transparent Au:Al Anodes. Journal of the Korean Physical Society, 2007, 50, 1327.  | 0.7 | 5         |
| 87 | Realâ€īme Correlation Detection via Online Learning of a Spiking Neural Network with a<br>Conductiveâ€Bridge Neuron. Advanced Electronic Materials, 2022, 8, .   | 5.1 | 5         |
| 88 | Capacitor-less memory-cell fabricated on nanoscale unstrained Si layer on strained SiGe<br>layer-on-insulator. Applied Physics Letters, 2010, 96, 163508.  | 3.3 | 4         |
| 89 | Effect of interface chemical properties on nonvolatile memory characteristics for small-molecule<br>memory cells embedded with Ni nano-crystals surrounded by NiO. Current Applied Physics, 2010, 10,<br>e32-e36.  | 2.4 | 4         |
| 90 | Effect of Organic Additive on Surface Roughness of Polycrystalline Silicon Film after Chemical<br>Mechanical Polishing. Japanese Journal of Applied Physics, 2010, 49, 010216.   | 1.5 | 4         |

| #   | Article   | IF  | CITATIONS |
|-----|---|-----|-----------|
| 91  | Effect of Small-Molecule Layer Thickness on Nonvolatile Memory Characteristics for Small-Molecule<br>Memory-cells. Electrochemical and Solid-State Letters, 2011, 14, H277.   | 2.2 | 4         |
| 92  | Capacitor-less memory cell fabricated on nano-scale strained Si on a relaxed SiGe layer-on-insulator.<br>Semiconductor Science and Technology, 2013, 28, 045001.  | 2.0 | 4         |
| 93  | Oxygen ion drift-driven dual bipolar hysteresis curves in a single Pt/Ta2O5â^'x/TiOxNy framework.<br>Applied Physics Letters, 2013, 103, 183510.  | 3.3 | 4         |
| 94  | High-stability transparent amorphous oxide TFT with a silicon-doped back-channel layer. Journal of the Korean Physical Society, 2014, 65, 1174-1178.  | 0.7 | 4         |
| 95  | Conductive-bridging random-access memory cell fabricated with a top Ag electrode, a polyethylene oxide layer, and a bottom Pt electrode. Journal of the Korean Physical Society, 2014, 64, 949-953.   | 0.7 | 4         |
| 96  | Nanoscale CuO solid-electrolyte-based conductive-bridging, random-access memory cell with a TiN<br>liner. Journal of the Korean Physical Society, 2018, 72, 116-121.  | 0.7 | 4         |
| 97  | Doping-less tunnel field-effect transistors by compact Si drain frame/Si0.6Ge0.4-channel/Ge source. AlP<br>Advances, 2021, 11, 045007.  | 1.3 | 4         |
| 98  | Super fine cerium hydroxide abrasives for SiO2 film chemical mechanical planarization performing scratch free. Scientific Reports, 2021, 11, 17736.   | 3.3 | 4         |
| 99  | Etch characteristics of magnetic tunnel junction materials using H <sub>2</sub> /NH <sub>3</sub><br>reactive ion beam. Nanotechnology, 2021, 32, 055301.  | 2.6 | 4         |
| 100 | Selectivity Enhancement in the Removal of SiO2 and Si3N4 Films with Addition of Triethanolamine in a<br>Ceria Slurry during Shallow Trench Isolation Chemical Mechanical Polishing. Journal of the Korean<br>Physical Society, 2008, 53, 1337-1342.                       | 0.7 | 4         |
| 101 | Hole Mobility Enhancement in Strained SiGe Grown on Silicon-on-Insulator p-MOSFETs. Journal of the<br>Korean Physical Society, 2008, 53, 2171-2174.   | 0.7 | 4         |
| 102 | Biâ€Stable Resistance Generation Mechanism for Oxygenated Amorphous Carbonâ€Based Resistive<br>Randomâ€Access Memory. Advanced Electronic Materials, 2022, 8, .   | 5.1 | 4         |
| 103 | A multi-level capacitor-less memory cell fabricated on a nano-scale strained silicon-on-insulator.<br>Nanotechnology, 2011, 22, 315201.   | 2.6 | 3         |
| 104 | Effective multi-step Ge condensation process using intermittent SiO2 strip to obtain a high-Ge concentration and a thick Ge-on-insulator (GeOI) substrate for p-MOSFET. Journal of the Korean Physical Society, 2013, 62, 531-535.  | 0.7 | 3         |
| 105 | Dependence of nickel gettering on crystalline nature in as-grown Czochralski silicon wafer. Journal<br>of Crystal Growth, 2013, 365, 6-10.  | 1.5 | 3         |
| 106 | Enhanced Thermal Stability in Magnetic Random-Access Memory Cells With Free Layer Composed of<br>Multilayer Co/Pt Coupled to Co <sub>2</sub> Fe <sub>6</sub> B <sub>2</sub> With Interfacial<br>Perpendicular Magnetic Anisotropy. IEEE Magnetics Letters, 2019, 10, 1-5. | 1.1 | 3         |
| 107 | Surface-Tensile-Stress Induced Polishing-Voids Suppression via H2O2 Oxidizer Effect in Cross-Point<br>Phase-Change-Memory-Cells. ECS Journal of Solid State Science and Technology, 2019, 8, P667-P672.   | 1.8 | 3         |
| 108 | Extremely high photoconductivity ultraviolet-light sensor using amorphous In–Ga–Zn–O<br>thin-film-transistor. Journal of the Korean Physical Society, 2021, 78, 1221-1226.  | 0.7 | 3         |

| #   | Article   | IF  | CITATIONS |
|-----|---|-----|-----------|
| 109 | Sputterâ€grown GeTe/Sb 2 Te 3 superlattice interfacial phase change memory for low power and<br>multiâ€levelâ€cell operation. Electronics Letters, 0, , .   | 1.0 | 3         |
| 110 | Hole Mobility Behavior in Strained SiGe-on-SOI p-MOSFETs. ECS Transactions, 2008, 13, 345-350.  | 0.5 | 2         |
| 111 | Effect of 8-hydroxy-quinolinato lithium thickness on the power conversion efficiency of polymer photovoltaic cells. Journal of the Korean Physical Society, 2013, 62, 490-495.  | 0.7 | 2         |
| 112 | Effect of β-cyclodextrin and Citric Acid on Chemical Mechanical Polishing of Polycrystalline<br>Ge2Sb2Te5in H2O2Containing Slurry. ECS Journal of Solid State Science and Technology, 2013, 2,<br>P299-P304.                            | 1.8 | 2         |
| 113 | Dielectric function of Si1â^'xGex films grown on silicon-on-insulator substrates. Journal of Applied Physics, 2014, 115, 233707.  | 2.5 | 2         |
| 114 | Effect of nanohole structure on pyramid textured surface on photo-voltaic performance of silicon solar cell. Journal of Applied Physics, 2014, 116, 084511.   | 2.5 | 2         |
| 115 | Effect of donor weight in a P3HT:PCBM blended layer on the characteristics of a polymer photovoltaic cell. Journal of the Korean Physical Society, 2015, 66, 1720-1725.   | 0.7 | 2         |
| 116 | Surface-tensile-stress induced polishing-voids in cross-point phase-change-memory cells: corrosion mechanism and solution. Semiconductor Science and Technology, 2019, 34, 065002.  | 2.0 | 2         |
| 117 | Dislocation sink annihilating threading dislocations in strain-relaxed<br>Si <sub>1â^'<i>x</i></sub> Ge <i><sub>x</sub></i> layer. Nanotechnology, 2020, 31, 12LT01.  | 2.6 | 2         |
| 118 | Impact of wet ceria abrasive size on initial step height removal efficiency for Isolated SiO2 film chemical mechanical planarization. Journal of the Korean Physical Society, 2021, 78, 51-57.  | 0.7 | 2         |
| 119 | Self-stopping slurry for planarizing extremely high surface film topography in nanoscale semiconductor devices. Journal of the Korean Physical Society, 2021, 79, 44-48.  | 0.7 | 2         |
| 120 | Design of n <sup>+</sup> -base width of two-terminal-electrode vertical thyristor for cross-point memory cell without selector. Nanotechnology, 2021, 32, 14LT01.   | 2.6 | 2         |
| 121 | Bidirectional Electric-Induced Conductance Based on GeTe/Sb2Te3 Interfacial Phase Change Memory for Neuro-Inspired Computing. Electronics (Switzerland), 2021, 10, 2692.  | 3.1 | 2         |
| 122 | Fenton Reaction for Enhancing Polishing Rate and Protonated Amine Functional Group Polymer for<br>Inhibiting Corrosion in Ge1Sb4Te5 Film Surface Chemical-Mechanical-Planarization. Applied Sciences<br>(Switzerland), 2021, 11, 10872. | 2.5 | 2         |
| 123 | Layerâ€dependent effects of interfacial phase change memory for an artificial synapse. Physica Status<br>Solidi - Rapid Research Letters, 0, , .  | 2.4 | 2         |
| 124 | Polymer link breakage of polyimide-film-surface using hydrolysis reaction accelerator for enhancing chemical–mechanical-planarization polishing-rate. Scientific Reports, 2022, 12, 3366.   | 3.3 | 2         |
| 125 | Scavenger with Protonated Phosphite lons for Incredible Nanoscale ZrO2-Abrasive Dispersant<br>Stability Enhancement and Related Tungsten-Film Surface Chemical–Mechanical Planarization.<br>Nanomaterials, 2021, 11, 3296.              | 4.1 | 2         |
| 126 | Optimal Channel Ion Implantation for High Memory Margin of Capacitor-Less Memory Cell Fabricated<br>on Fully Depleted Silicon-on-Insulator. Japanese Journal of Applied Physics, 2010, 49, 036507.                                      | 1.5 | 1         |

| #   | Article  | IF  | CITATIONS |
|-----|--|-----|-----------|
| 127 | High polishing selectivity ceria slurry for formation of top electrode in spin-transfer torque magnetic random access memory. Thin Solid Films, 2012, 522, 212-216.  | 1.8 | 1         |
| 128 | Effect of a thermally evaporated bis (2-methyl-8-quninolinato)-4-phenylphenolate cathode buffer layer<br>on the performance of polymer photovoltaic cells. Journal of the Korean Physical Society, 2012, 61,<br>507-512. | 0.7 | 1         |
| 129 | Effect of NH3 plasma passivation on the electrical characteristics of a nanolaminated ALD HfAlO on<br>InGaAs MOS capacitor. Journal of the Korean Physical Society, 2015, 66, 1885-1888.                                 | 0.7 | 1         |
| 130 | Multi-level resistance uniformity of double pinned perpendicular magnetic-tunnel-junction spin-valve depending on top MgO barrier thickness. AlP Advances, 2020, 10, .   | 1.3 | 1         |
| 131 | A bow-free freestanding GaN wafer. RSC Advances, 2020, 10, 21860-21866.  | 3.6 | 1         |
| 132 | Enhanced performance of polymer solar cells using selective silver nanocrystal morphology. Journal of the Korean Physical Society, 2021, 79, 49.   | 0.7 | 1         |
| 133 | Nonvolatile Hybrid Memory Cell Embedded with Ni Nanocrystals in Poly(3-hexylthiophene). Japanese<br>Journal of Applied Physics, 2012, 51, 120202.  | 1.5 | 1         |
| 134 | Two-terminal vertical thyristor using Schottky contact emitter to improve thermal instability. Nano Futures, 0, , .  | 2.2 | 1         |
| 135 | Surface Transformation of Spin-on-Carbon Film via Forming Carbon Iron Complex for Remarkably<br>Enhanced Polishing Rate. Nanomaterials, 2022, 12, 969.   | 4.1 | 1         |
| 136 | Effect of Au Nanocrystals Embedded in Conductive Polymer on Non-volatile Memory Window.<br>Materials Research Society Symposia Proceedings, 2008, 1071, 1.   | 0.1 | 0         |
| 137 | Fabricated nonvolatile memory with Ag nano-crystals embedded in PVK. , 2010, , .   |     | 0         |
| 138 | Small-Molecule Nonvolatile Memory Cells Embedded with Ti Nanocrystals Surrounded by TiO\$_{2}\$<br>Tunneling Barrier. Applied Physics Express, 2011, 4, 105003.  | 2.4 | 0         |
| 139 | Dependence of Ag Film Thickness on Ag Nanocrystals Formation to Fabricate Polymer Nonvolatile<br>Memory. IEICE Transactions on Electronics, 2011, E94-C, 850-853.  | 0.6 | Ο         |
| 140 | Effect of MeV nitrogen ion implantation on the resistivity transition in Czochralski silicon wafers.<br>Journal of the Korean Physical Society, 2012, 61, 1981-1985.   | 0.7 | 0         |
| 141 | Relationship of Free Surface Area with Oxygen Concentration in Silicon Ingot Grown by Czochralski<br>Method for High Efficiency Solar Cells. Journal of the Korean Physical Society, 2020, 77, 940-944.                  | 0.7 | Ο         |
| 142 | Nonvolatile Polymer Memory-Cell Embedded with Ni Nanocrystals Surrounded by NiO in Polystyrene.<br>IEICE Transactions on Electronics, 2013, E96.C, 699-701.  | 0.6 | 0         |
| 143 | Two-step hydrogen-ion implantation annihilation of threading dislocation defects in strain-relaxed Si0.7Ge0.3. Journal of the Korean Physical Society, 2021, 79, 1151-1156.  | 0.7 | 0         |
| 144 | Perpendicular-spin-transfer-torque magnetic-tunnel-junction neuron for spiking neural networks<br>depending on the nanoscale grain size of the MgO tunnelling barrier. Materials Advances, 2022, 3,<br>1587-1593.        | 5.4 | 0         |